Optimization of the Straightness Measurements on Rough Surfaces by Monte Carlo Simulation

François Hennebelle, Thierry Coorevits, Maxence Bigerelle

Optimization of the Straightness Measurements on Rough Surfaces by Monte Carlo Simulation

F. Hennebelle,[1,2] T. Coorevits,[3] and M. Bigerelle[4]

[1]Laboratoire d'Electronique, Informatique et Image, UMR CNRS 6306, Université de Bourgogne, Auxerre Cedex, France
[2]Centre Technique des Industries Mécaniques (CETIM), Pôle Expertise, Métrologie, Etalonnage, Senlis, France
[3]Laboratoire de Mécanique de Lille, UMR CNRS 8107, Arts et Métiers ParisTech, Lille Cedex, France
[4]Equipe Matériaux, Surfaces et Mise en forme, TEMPO/LAMIH CNRS-UVHC 8530, Université de Valenciennes et du Hainaut-Cambraisis, Valenciennes, France

Summary: The straightness error of a coordinate measuring machine (CMM) is determined by measuring a rule standard. Thanks to a reversal technique, the straightness uncertainty of the CMM is theoretically dissociated from the straightness uncertainty of the rule. However, stochastic variations of the whole measurement system involve uncertainties of the CMM straightness error. To quantify these uncertainties, different sources of stochastic variations are listed with their associated probability density functions. Then Monte Carlo methods are performed first to quantify error and secondly to optimize measurement protocol. It is shown that a 5-measurement distance from 0.1 mm to each measurement coordinate allows a double reduction of uncertainties, principally due to the rule roughness amplitude ($R_a = 0.35$ μm) and because this optimal distance of 0.1 mm is equal to the autocorrelation length of the rule roughness. With this optimal configuration, the final uncertainly on the straightness error of the CMM studied is less than 1 μm on the whole evaluated length of the rule (1 m). An algorithm, including Probe Tip Radius of the CMM and surface roughness of the piece, is finally proposed to increase CMM reliability by minimizing error measurements due to surface roughness of the measured piece. SCANNING 36: 161–169, 2014. © 2013 Wiley Periodicals, Inc.

Key words: metrology, roughness, straightness, uncertainties, Monte Carlo

Address for reprints: F. Hennebelle, Laboratoire d'électronique, Informatique et Image, UMR CNRS 6306, Université de Bourgogne, Auxerre Cedex, France
E-mail: francois.hennebelle@u-bourgogne.fr

Introduction

Straightness of a piece is often a basic requirement in order for a machine to function correctly and/or produce fault-free parts. This straightness is often measured daily by a coordinate measuring machine (CMM) in many industries, for example, members, rollers, pipes, machine ends, machine runners, and conveyors. Straightness measurements are also carried out for bearing positions in, for example, diesel engines. For the CMM, the Geometrical Product Specification standard (GPS) defines straightness as a two-dimensional geometric tolerance that controls how much a feature can deviate from a straight line (NF E 10-101, '88; NF E 11-151, 2003). Therefore, for a machine, the straightness default along an axis represents the deviation from this axis in the directions perpendicular to the displacement.

One of the metrological problems with CMMs arises in straightness errors along the horizontal and vertical axes. Determining the straightness defaults of a CMM can be performed using a rule as a geometric standard. However, the rules themselves incur straightness defaults that will be added to CMM errors. The separation of the straightness default of the rule and those of the machine is commonly performed by means of reversal procedures (Cayère, '56; Whitehouse, '76): to measure the straightness of the rule (the EABF plane in Fig. 1), a first measurement is carried out along the longitudinal axis (x_{piece}), and a second one after turning the rule to this axis (a 180° rotation).

Nevertheless, it remains impossible to locate precisely the same set of coordinates (x_{piece}, y_{piece}, z_{piece}) in the piece-coordinate system after processing to the rule rotation. This impossibility is due to two categories of uncertainty. The first one can be modeled, taking into account deterministic considerations such as modeling the flexion of the rule under its own weight. The second uncertainty is stochastic in nature and is directly linked to

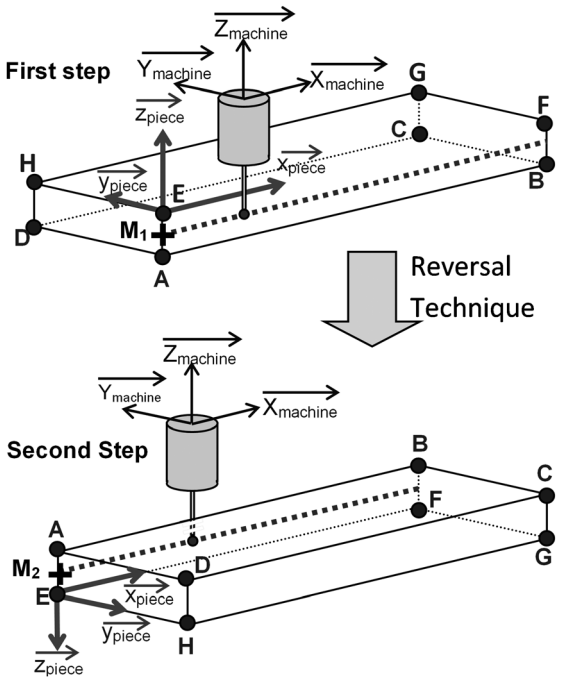

Fig 1. Description of the measurements on the rule.

the local uncertainties in the (x_{piece}, y_{piece}, z_{piece}) location. The stochastic errors can be linked into two classes of errors: the position errors on the plane, i.e. the (x_{piece}, z_{piece}) coordinate location, and the altitude position error along the y_{piece} axis. After some investigations, it can be determined that the (x_{piece}, z_{piece}) errors are reduced to three stochastic errors: the lack of precision in repositioning between the two steps of the reversal procedure, uncertainties on the target location error owing to the numerical control, and machine repeatability. The error in determining the straightness error of the machine in the $x_{machine}$, $y_{machine}$ plane is influenced by the rule's deformation due to climatic changes that induce thermal strains. The y_{piece} error is principally based on the statistical variations of the surface topography due to the roughness of the rule, thermal strain, and machine repeatability. The aim of this paper is to build a method to reduce the uncertainty about the straightness determination by taking account of these sources of errors. A Monte Carlo simulation (JCGM 100:2008; JCGM 101:2008; JCGM 102:2011) associated with an original protocol of measure is proposed to reduce drastically the uncertainties of the straightness evaluation. This study is also applicable when measuring in scanning mode (Savio, 2006; Pereira and Hocken, 2007).

Principle to Determine the Straightness of the Rule

To facilitate understanding, the faces are identified as follows (Fig. 1):

- The setting face corresponds to the AEHD face.
- The fitting face is the ABCD face in the first step and the EFGH face in the second step of the straightness measurement.

Generality

The measures are realized in two steps (Fig. 1), namely:

- A direct measurement along the length of the rule.
- A measurement done with a similar protocol to the first step, after a 180° rotation of the rules around its longitudinal axis. As a consequence, the theoretical coordinates are the same from one position to another.

Positioning the Rule on the Machine

A repository reproducible and a mechanical system for positioning the rule must be defined to limit its distortion and thus minimize the positioning errors. Moreover, the determination of the repository must be the same for both steps of measurements (before and after reversal).

The rule is fixed on three points in order to have an isostatic system. The three points of the fitting position must be provided such that two points are as close as possible to the measuring face in the two steps (Fig. 2). Also, these points are positioned at the 2/9 of the rule length in order to limit the flexion of the rule under its own weight. Thus, in the first step, the fitting points P1 and P3 are aligned, and are set closer to the measuring face. It is better to move the point P3 to that place in the middle of the rule to avoid deformation of the measuring face between the two steps A gauge block is tentatively fixed against the setting face. Thus, when turning, minimal contact against the gauge block is needed to ensure positioning along the longitudinal axis of the

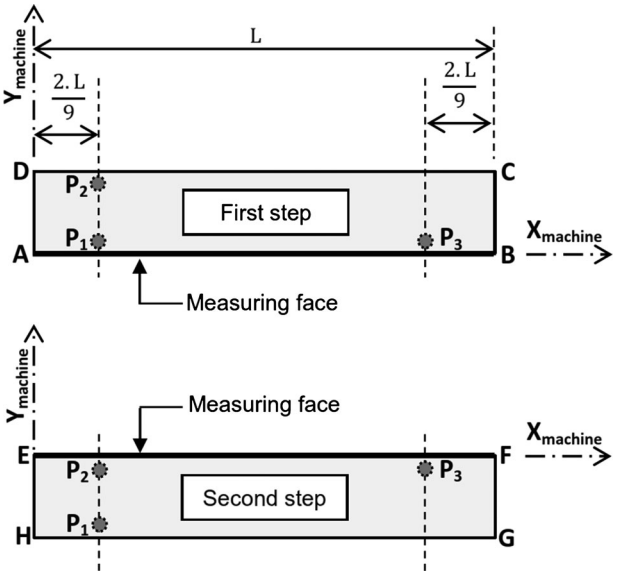

Fig 2. Location of the fitting P1–P3 points of the rule.

rule. By contrast, between the two steps, the fitting face changes, as specified above. For these two reasons the setting and fitting faces must provide honing and polishing to minimize positioning errors. After turning the rule (second step), in order to realize a good fitting position, point P3 must be moved, and P2 and P3 aligned and set closer to the measuring face.

Formalism

Figure 3 shows the calculation principle to determine the straightness either of the rule $r(x)$ or of the machine $m(x)$, using the reversal technique.

Nevertheless, it is necessary to ask three sign conventions:

- If the point on the trajectory of the machine moves to Y positive, then the default is counted positively and is denoted $+m(x)$.
- A bump of the rule is interpreted as a positive default that is denoted as $+r(x)$.
- If the sensor sinks, this information is positive
- In the first step, the comparator records: $e_1(x) = m(x) + r(x)$.
- In the second step, the comparator records: $e_2(x) = -m(x) + r(x)$.
- The half-sum and half-difference provide $r(x)$ and $m(x)$.

Errors Classifications in the Straightness Determination of the Rule

Positioning Error

To determine the straightness of the rule by a reversal technique, the precise repositioning of the rule is essential in the measurement process. Consequently, the sources of errors in the repositions must be listed and quantified.

There are four major positioning errors:

- A low error in angular position of the rule (Z_{axis}). This error causes a rotation curve of the straightness curve, similar to a perpendicular error (Ekinci and Mayer, 2007). This error can be suppressed by removing the slope of the straightness.
- A positioning error by translation of the CMM probe head along the transversal axis of the rule (z_{axis}). This error only causes a simple translation of the straightness curve without affecting its shape.
- A position error of the rule by translation of the CMM probe head along the longitudinal axis (x_{axis}). In this situation, the roughness of the rule produces most of the errors. In fact, the amplitude of the roughness will create a measurement noise on the measurement of straightness. The positioning according to this longitudinal axis must be achieved with maximum accuracy.
- A position error of the rule by vertical translation of the CMM probe head (along the thickness of the rule). This error is due to the different roughness of the rule at the contact (fitting position—Fig. 2, points P1–P3) and at the flexion of the rule under its own weight (position of coordinates relative to the pitch line).

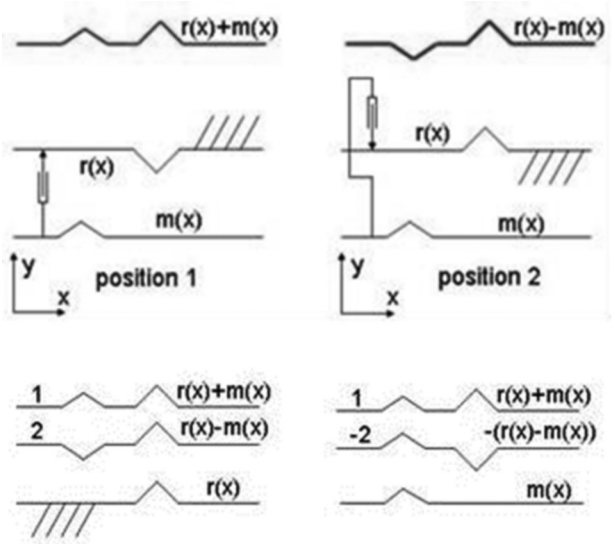

Fig 3. Principle to process the measurements

Deformation Caused by Thermal Strains Fluctuations

Potential evolution of the straightness, especially during the climatic changes, can induce thermal strains and thus a modification of the system coordinates of the rules.

Quantification Determination of Élémentary Defaults

The CMM Measures

The straightness of the machine depends on the plane (x, y). The CMM characterized is a Leitz™ PMM-C 1000P (24 12 10), Hexagon Metrology Group, which means that its useful dimensions are, respectively, 2.4 m on the x, 1.2 m on the y, and 1 m on the z-axis. This CMM is equipped with a continuous High-Speed-Scanning probe head LSP-S4. This CMM is commercialized by the Hexagon Metrology Group. The rule used for determining the straightness is made of steel; its different faces provide honing and polishing, and it is 1 m long. The room is controlled for temperature and humidity at $20 \pm 1^{\circ}$C. The rule and the CMM are controlled for temperature in order to make necessary corrections automatically. A step in measuring straightness takes about 20 min. There are 101 measured sites,

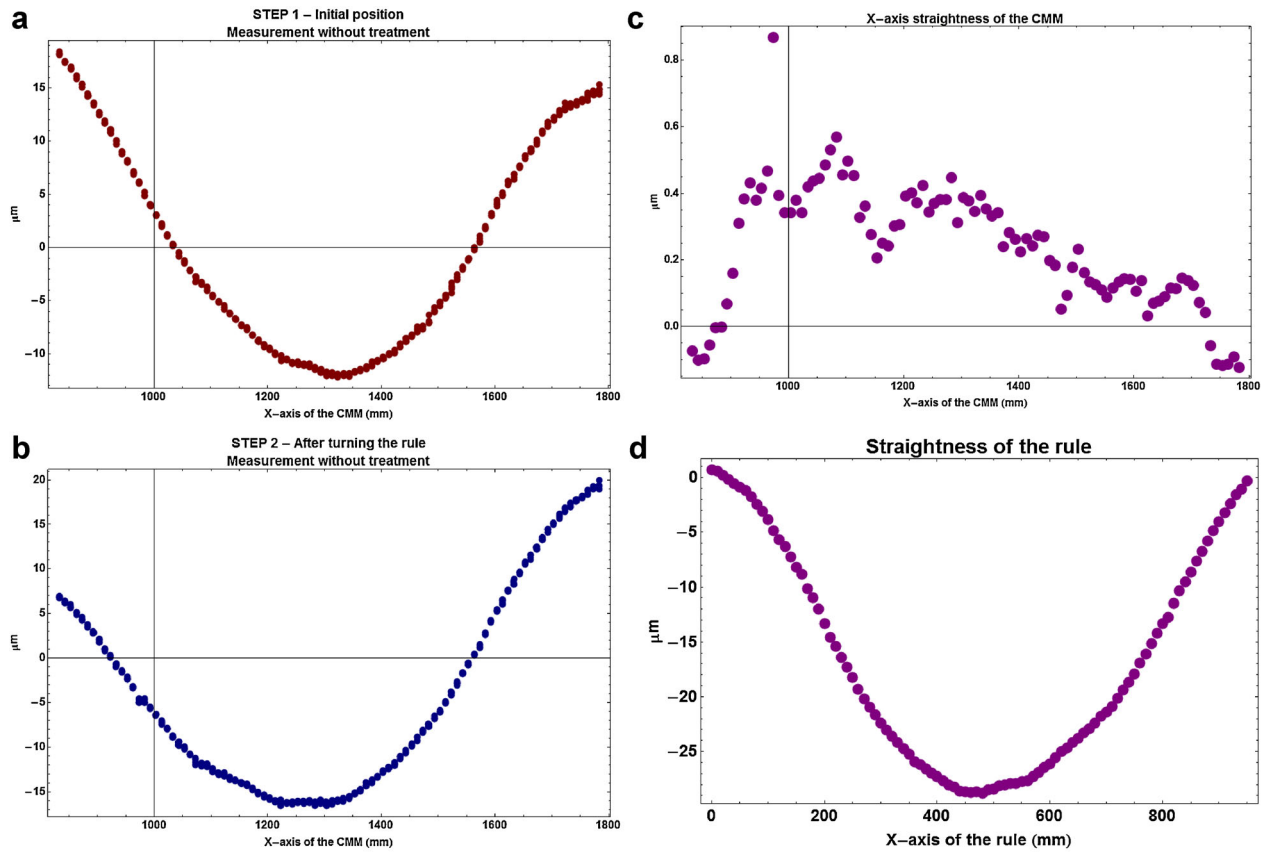

Fig 4. Straightness measurement of the rule along x-axis (**a**) and y one (**b**) and the corresponding computation of the CMM straightness in x-axis (**c**)) and y one (**d**).

and five points are measured by site. Figure 4 represents the measurements of (a) the straightness on x-axis before the reversal technique and (b) after the reversal technique.

Defaults of Positioning on Each Axis

To determine these positioning errors, a repository is defined, the setting face is measured several times, and the position along the longitudinal axis from a point of this plan is assessed. Along the longitudinal axis, the errors of setting position are experimentally estimated at ± 0.1 mm (uniform distribution). This point can be built, for example, as the intersection of this plane with the theoretical measured line. Along the vertical axis, the fitting errors (vertical positioning errors) are estimated experimentally at ± 0.02 mm (uniform distribution). This error takes account of the deformation of the rule, especially the flexion of the rule under its own weight and the vertical error due to the thickness variation of the rule.

Roughness Default Including CMM Tip Radius Integration

The roughness of the rule can be seen as a local default of rule geometry. The surface of the rule provides honing and polishing. In fact, the roughness impacts directly the repeatability of the straightness measurements. With these mechanical treatments, the roughness of the rule, seen by the CMM, has a total roughness of R_t equal to less than one micrometer (more precisely $R_a = 0.35$ µm on both transversal and longitudinal directions). It is only with such treatment that it will be possible to obtain uncertainties of about 1 µm. To determine the influence of the rough surface of the rule on the measurement of straightness, it is

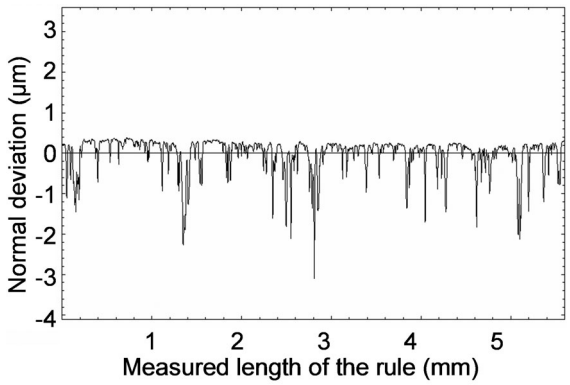

Fig 5. Roughness profile of the rule surface along the X-axis of the rule.

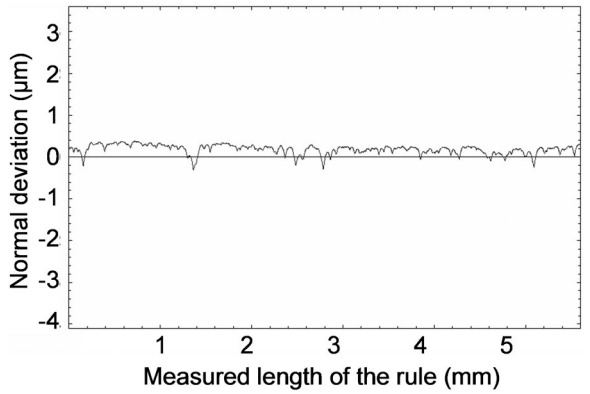

Fig 6. Roughness profile of the rule surface after morphological filtering representing the tip radius integration of the CMM probe head.

necessary to measure the roughness (Fig. 5) and simulate the tip integration due to the tactile measurement on the rule. Roughness profiles are measured by the mechanical profilometer; the tip radius is about a few micrometers. This tip radius is negligible in comparison with the ball of the stylus used for the straightness measurements. The stylus chosen for the straightness measurement on the CMM is a ball of 5 ml diameter. As the rule is measured on the CMM using a stylus with a ball of 5 ml, a morphological filtering (with a ball of 5 ml) (Bigerelle, '99; Wu, '99; Coorevits *et al*., 2004; Pawlus, 2004) is performed to simulate the apparent profile of the rule for the machine. It is therefore necessary to realize a morphological filtering with a ball of the same diameter (Fig. 6). The profile, after the morphological filtering is smoother than the initial profile; that is natural because this filtering is a dilatation of the profile with respect to a ball-shaped structuring element of a radius 2.5 ml. In Figures 5 and 6, normal deviations correspond to the heights of the measured profile. Figure 6 represents the profile obtained after filtering, which is measured by the machine.

Tracking Errors

The tracking measurements correspond to the deviation from the theoretical position in the two directions perpendicular to the measurement. The tracking errors are directly estimated on straightness measurements. The tracking errors in the vertical and longitudinal directions are represented on the histograms (experimental values; Figs. 7 and 8). The tracking errors are relatively slight (around 2 μm).

Statistical Considerations

By measuring multi-point features, the accuracy and repeatability of the feature will be optimized.

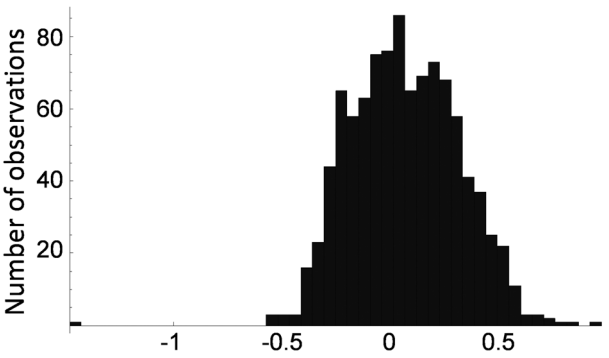

Fig 7. Tracking error (μm) along the longitudinal axis of the rule.

Measurement Repeatability

To quantify the machine repeatability on straightness measurements, 30 straightness measurements are done, following standard measurement protocol. All external conditions include keeping a constant temperature and rule position. The dispersion (standard deviation) is evaluated at about $\pm$ 0.1 μm on both X_{machine} and Z_{machine} axes on the CMM (Gaussian distribution).

Number of Located Points

A good strategy is to measure the same point several times, which allows averaging and reduces the measurement noise. In fact, the uncertainties on a measured point decrease if the number n of measurements increases according to the $1/\sqrt{n}$ rate. To make a compromise among a large number of measurement points, as well as to have an average effect and a reasonable time of measurement, five points seems to be a good choice. In fact, in using between four and six measurement points the gain in terms of uncertainty is less than 10%. With increasing measurement time and

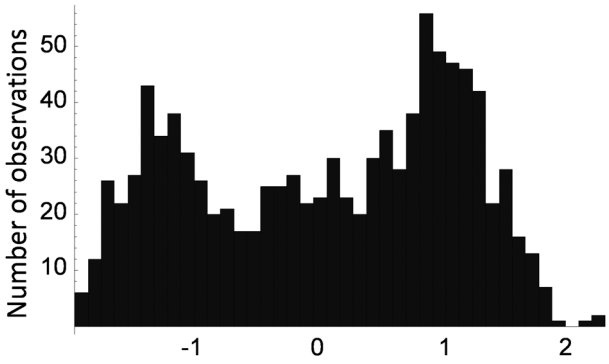

Fig 8. Tracking error (μm) along the vertical axis of the rule.

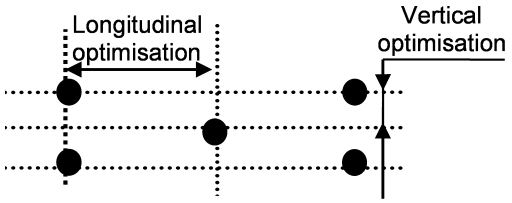

Fig 9. Distances that must be optimized.

the risk of thermal drift, it is wise to choose five measuring points.

Monte Carlo simulation

Presentation of the Monte Carlo Simulation Performed

A Monte Carlo simulation (Schwenke *et al*., 2000; Wilhelm *et al*., 2001; Gentle, 2003; Gustavo Gonzalez *et al*., 2005; Trapet, 2005; Dhanish *and* Mathew, 2006; Sanchez *and* Santillan, 2006) will be performed, which allows optimization of the coordinates measured. The goal of this Monte Carlo simulation is to identify the best the longitudinal and vertical position of the coordinates. To take account for different positioning problems, it was decided to locally distribute five points as the number 5 of a poker die (Fig. 9), which is relatively conventional in metrology. Thus, the estimated value of an altitude is the average of five localized altitudes, where the distance from the gravity center (center of the poker dice motif) to the four peripheral points must be optimized. Decreasing this distance, increasing the localization reduces the precision (altitudes are relatively the same due to stylus integration and similarity in roughness altitude). On the contrary, increasing this distance, reducing the localization yields greater precision. This distance is considered as optimal if the standard deviation computed from the five altitudes is minimal. In the simulation, this distance between two zones of five points is limited to 10 ml.

Presentation of the Monte Carlo Parameters

The various parameters interfering with the measurement (repeatability, tracking errors, positioning errors) have been assessed for the implemented process. These parameters are the sources of uncertainty. Each parameter is associated with a distribution, namely, a Gaussian is characterized by the mean and standard deviation, or a uniform law is characterized by an interval. Table I represents the parameters used in the simulation with the nature of the probability density function and their associated parameters.

The performed Monte Carlo Simulation

The simulation was performed as follows:

Thirty roughness profiles were determined experimentally for all the measuring surface of the rule (longitudinal and transverse measurements). For each profile, the following steps were completed as many times as the number of Monte Carlo simulations performed:

1. Simulate the possible variations to this profile when measured with the CMM, namely:

   - Dilatation of the profile with respect to a ball-shaped structuring element of a radius 2.5 ml, in order to generate a continuous profile.
   - Simulation of the measurement of the profile by a CMM; Theoretical points and measured points are not really the same due to resolution, repeatability, tracking errors, Thus, simulating the points actually measured for each simulation according to the draft produced for each parameter it recreates so much profiles as simulations.

   For example: consider an evaluation along the x-axis. To determine a simulated profile in the first step in the X-axis, $Y_{\text{simulate\_Step1}}(x)$ is also the theoretical y at the x position + positioning errors, where positioning errors are the sum of:

TABLE I Input parameters of the Monte Carlo simulation

N°	Error	PDF	PDF parameters
1	Positioning errors along X- or Y-axis (μm)	Uniform	$D = \pm 100$
2	Positioning errors along Z-axis (μm)	Uniform	$D = \pm 20$
3	CMM resolution (μm)	Uniform	$D = \pm 0.025$
4	CMM repeatability (μm)	Gaussian	Mu = 0, Std = 0.2
5	CMM tracking error along the X- or Y-axis (μm)	Uniform	$D = \pm 1$
6	CMM tracking error along the Z-axis (μm)	Uniform	$D = \pm 2$
7	Dilatation due to thermal expansion of the rule of 1 m long (L), d: distance position on the rule (μm)	Uniform	$D = \pm 5.75d/L$

D is the range of the uniform law and Mu and Sig the mean and the standard deviation of the Gaussian law.

- A random in an uniform distribution of the source of uncertainty number 3.
- A random in an uniform distribution of the source of uncertainty number 5.
- A random in the Gaussian distribution of the source of uncertainty number 4.

2. Generate the profile in a reversal technique. That is to say, restart the same operations as the previous step but shift the profile of a random value in a Gaussian distribution corresponding the possible gap, according to the considered direction (longitudinal or transversal).
   For example: consider an evaluation along the x-axis. To determine a simulated profile in the second step in the X-axis, $Y_{\text{simulate\_Step2}}(x)$ is also the theoretical y at the x position + positioning errors, where positioning errors are the sum of:

   - A random in an uniform distribution of the source of uncertainty number 1.
   - A random in an uniform distribution of the source of uncertainty number 3.
   - A random in an uniform distribution of the source of uncertainty number 5.
   - A random in an uniform distribution of the source of uncertainty number 7, which correspond to an evolution of temperature between this step and the previous.
   - A random in the Gaussian distribution of the source of uncertainty number 4.

3. Calculate the distances (normal deviation) between the respective coordinates of the two simulated profiles, and calculate the mean of the absolute value of the difference for the five local points.
   For example: consider an evaluation along the x-axis. $|Y_{\text{simulate\_Step2}}(x) - Y_{\text{simulate\_Step1}}(x)|$ is calculated, and the mean of the for the five local points is raised.
4. Thus, the vertical and horizontal distance between the points (on the five localized points) is optimized such that it minimizes the standard deviation of the normal deviation calculated.

For example: consider an evaluation along the x-axis. The optimum corresponds to the minimum of the previous calculation when varying the distance along x between the five local points.

To summarize, the profile is shifted a certain value, the difference between the point on the initial profile and the offset profile is calculated. The goal is to minimize the standard deviation of this difference in the longitudinal (Fig. 10) and the transversal (Fig. 11) direction. Thus, by the Monte Carlo process, the optimum disposition of points was obtained (Fig. 12). The setting face in the longitudinal direction causes a

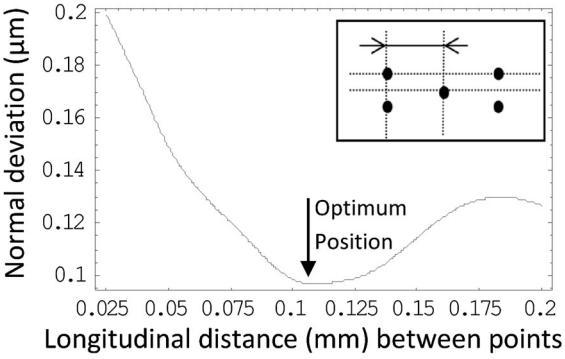

Fig 10. Plot of the straightness versus the longitudinal spacing of the five local measurements.

positioning error of ± 0.1 mm in this direction. This analysis gives evidence that this parameter is the most influent on the measurement's uncertainties. The optimal distance between the points in the longitudinal direction is 0.1 mm ± 0.02 mm (Fig. 10). In the transversal direction, the optimal distance is 0.05 mm ± 0.015 mm, and the most influential parameter is the roughness of the rule (Fig. 11). The following serves to explain these optimal values. As the hypothetical explanation at the beginning of this paragraph noted, the data points must be sufficiently far from the gravity

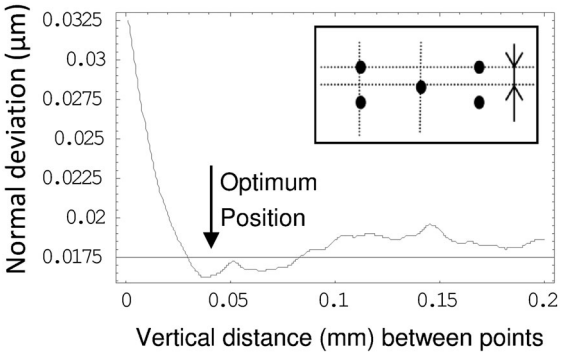

Fig 11. Plot of the straightness versus vertical spacing of the five local measurements.

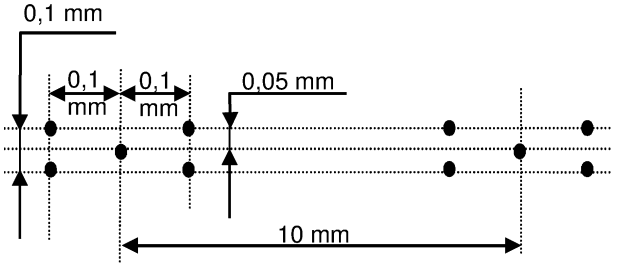

Fig 12. Optimal localizations of coordinate measurement along the rule (X-axis).

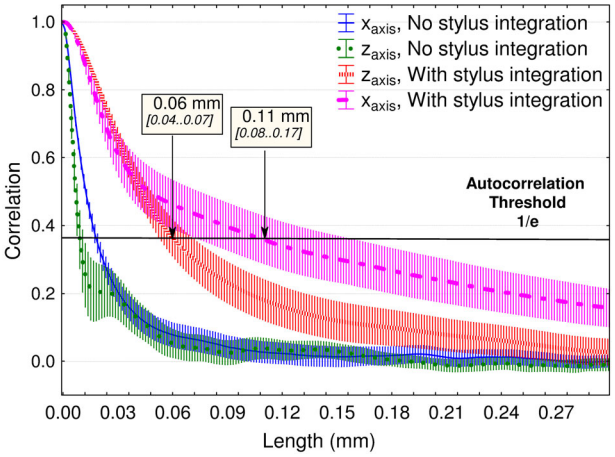

Fig 13. Plot of the averaged autocorrelation functions (with their 95% confidence intervals) of the roughness rules in both X_{axis} and Y_{axis} directions with and without stylus integration of the CMM Probe.

center to integrate the variability of the roughness. More precisely, the effect of the roughness amplitude of each coordinate must be independent of the roughness of the gravity center of the poker dice shape. In surface topography, this independence is linked to the autocorrelation function. As a consequence, the autocorrelation functions of 37 roughness profiles in both directions (along x_{axis} and y_{axis}) are computed before and after the stylus integration filtering. The autocorrelation functions are averages that allows us to compute their errors. Figure 13 represents these four averaged autocorrelation functions. First, the stylus integration has the effect of increasing the autocorrelation length. This is due to the stylus simulation, which produces a smoothing of the surface topography that is linked to an increase of the autocorrelation length. Secondly, the autocorrelation length (computed at the usual threshold of $1/e$–0.37) is equal to 0.06 mm [0.04–0.07] along z_{axis} and 0.11 mm [0.08–0.17] along x_{axis}. These values are equals to the value of the optimal distance (0.1 mm $\pm$ 0.02 mm (Fig. 10) along x_{axis} and 0.05 mm $\pm$ 0.015 mm along z_{axis} (Fig. 11). Similar approached values can be analytically obtained by considering the rule (straightedge) having a Gaussian roughness. We then filter the honed surfaces by a morphological filter to obtain a Gaussian-shape from which roughness amplitude can be extracted. The autocorrelation length is then obtained by a simple trigonometric calculation of the chord of a circle determined by the radius and the radius minus the roughness. For a ball radius of D, with a roughness amplitude R micrometers, the autocorrelation of 95% independence should occur at the $\sqrt{D^2-(D-3R)^2}$ distance and give 0.07 mm along z_{axis} and 0.12 mm along x_{axis}. This outcome, i.e. the optimal distance is equal to the autocorrelation length of the rule roughness after stylus integration, means that the optimal distance depends on:

- The stylus radii of the CMM probe.
- The roughness of the rules.

The other CMM errors can be minimized in choosing optimal distances. Then, a procedure to determine the optimal distance of the poker dice position can by proposed in the following four steps:

- *Step 1*. Record profiles on longitudinal and transversal of the rules.
- *Step 2*. Apply a stylus integration algorithm on the profile, taking into account the radius of the CMM probe.
- *Step 3*. Compute the autocorrelation function.
- *Step 4*. Compute the longitudinal and transversal autocorrelation lengths at the threshold of $1/e$. These values provide the characteristic distance of the poker dice shape.

This original methodology could be applied generically to all CMM measurements on industrial pieces with rough surface (even for low surface roughness, R_a = 0.35 μm in our study), in order to increase CMM reliability and thereby minimize error measurements.

Conclusions

The reversal technique to determine straightness is simple, but its implementation is difficult. The roughness of the rule and the quality of repositioning are essential to the quality of the result. The causes of uncertainty are essentially: the roughness, the setting, the tracking error, the sensor, the repeatability of the machine, and the uncertainties on the measurement of the axis. This study has greatly optimized this measure and has allowed calculation of the straightness with an uncertainty of about one micrometer on a length of one meter. This study was conducted as part of the first accreditation in France MMT (Hennebelle *et al*., 2011). There are many potential applications in the field of microscopy. Indeed, it is possible, with a similar technique to characterize the straightness of a table moving in the optical microscope, for example, to conduct metrology on very small pieces.

References

Bigerelle M. 1999. Caractérisation géométrique des surfaces et interfaces—Application en métallurgie [Thesis]. Lille, France: ENSAM.

Cayère M. 1956. Mesure des défauts d'une règle-étalon, Extraits de Manipulation de Métrologie mécanique, Publié en polycopié de décembre 1956 à mai 1957 par l'Ecole Libre d'Apprentissage de Grenoble.

Coorevits T, Rousset N, Vincent R. 2004. Uncertainties on coordinate measuring machine: part and method, Proceedings of the 11th international congress of metrology, Toulon, France, 21–24 October 2003.

Dhanish PB, Mathew J. 2006. Effect of CMM point coordinate uncertainty on uncertainties in determination of circular features. Measurement 39:522–531.

Ekinci O, Mayer JRR. 2007. Relationships between straightness and angular kinematic errors in machines. Int J Mach Tools Manuf 47:1997–2004.

Gentle JE. 2003. Random number generation and Monte Carlo methods. Series: statistics and computing. 2nd edition. New York: Springer.

Gustavo Gonzalez A, Angeles Herrador M, Asuero AG. 2005. Uncertainty evaluation from Monte-Carlo simulations by using Crystal–Ball software. Accred Qual Assur 10:149–154.

Hennebelle F, Coorevits T, Sessa P. 2011. Presentation of the first COFRAC accreditation on coordinate measuring machine, Proceedings of the 15th international congress of metrology, Paris, France, October 3–6, 2011.

JCGM 100. 2008. Guide to the expression of uncertainty in measurement.

JCGM 101. 2008. Evaluation of measurement data—Supplement 1 to the "Guide to the expression of uncertainty in measurement"—Propagation of distributions using a Monte Carlo method.

JCGM 102. 2011. Evaluation of measurement data—Supplement 2 to the "Guide to the expression of uncertainty in measurement"—Extension to any number of output quantities. JCGM 102:2011.

NF E 10-101, février. 1988. ISO 230-1:2012, Test code for machine tools—Part 1: geometric accuracy of machines operating under no-load or quasi-static conditions.

NF E 11-151: Décembre. 2003. Machines à mesurer tridimensionnelles à portique, Représentation des corrections de géométrie.

Pawlus PP. 2004. Mechanical filtration of surface profiles Measurement 35:325–341.

Pereira PH, Hocken RJ. 2007. Characterization and compensation of dynamic errors of a scanning coordinate measuring machine. Precision Eng 31:22–32.

Sanchez J, Santillan S. 2006. Simpler approach to virtual multiaxis machines: fundamentals. Measurement 39:352–370.

Savio E. 2006. Uncertainty in testing the metrological performances of coordinate measuring machines. Ann CIRP 55:535–538.

Schwenke H, Siebert BRL, Wäldele F, Kunzmann H. 2000. Assessment of uncertainties in dimensional metrology by Monte Carlo simulation: proposal of a modular and visual software. Ann CIRP 49:395–398.

Trapet E. 2005. Measuring with vision systems: industry standards for acceptance and verification tests, Proceedings of the 3rd EMVA Business Conference, Palermo.

Whitehouse DJ. 1976. Some theoretical aspects of error separation techniques in surface metrology. J Phys E 9:531–536.

Wilhelm RG, Hocken R, Schwenke H. 2001. Task specific uncertainty in coordinate measurement. Ann CIRP 50:553–563.

Wu JJ. 1999. Spectral analysis for the effect of stylus tip curvature on measuring rough profiles. Wear 230:194–200.